Anthricin-induced caspase-dependent apoptosis through IGF1R/PI3K/AKT pathway inhibition in A549 human non-small lung cancer cells

BO-RAM PARK[1], SEUL AH LEE[2], SUNG MIN MOON[3] and CHUN SUNG KIM[2]

[1]Department of Dental Hygiene, Chodang University, Muan-ro, Muan-eup, Muan 534-701;
[2]Department of Oral Biochemistry, College of Dentistry, Chosun University, Dong-gu, Gwangju 501-759;
[3]CStech Research Institute, Gwangju 61007, Republic of Korea

Received October 31, 2017; Accepted March 23, 2018

DOI: 10.3892/or.2018.6333

Abstract. Anthricin (deoxypodophyllotoxin) is a major lignan in *Anthriscus sylvestris* and possesses many bioactivities such as antiproliferative, antitumor, anti-platelet aggregation, antiviral and anti-inflammatory actions. However, the anticancer effects of anthricin on A549 human non-small cell lung cancer cells and potential molecular mechanisms remain unknown. Therefore, we investigated the anticancer effect of anthricin and the underlying mechanism in A549 cells. Anthricin (10-200 nM) inhibited the viability of A549 cells in a dose- and time-dependent manner. Moreover, anthricin-induced apoptosis was confirmed by live and dead assay, 4,6-dianmidino-2-phenylindole staining, and flow cytometric analysis. In addition, anthricin induced cell cycle arrest at the G2/M phase through suppression of the expression of cell cycle cascade proteins, Cdc2 and Cdc25C. Furthermore, it induced the expression of caspase-related proteins and significantly suppressed the phosphorylation of insulin-like growth factor 1 receptor (IGF1R), PI3K and Akt. Anthricin significantly inhibited tumor growth without any significant change in the body weight of mice in A549 tumor xenograft BALB/c nude mice. Anthricin induced caspase-dependent apoptosis through the IGF1R/PI3K/Akt signaling pathway in A549 cells.

Introduction

Lung cancer is the leading cause of cancer-related deaths worldwide, with a 5-year survival rate of ~15% (1,2). Based on cell size, lung cancer is classified into small cell lung cancer (SCLS), which accounts for 15-20% of all lung cancers, and non-small cell lung cancer (NSCLC), which accounts for the remaining ~80%. Adenocarcinoma accounts for 40% of NSCLC, and the prognosis is poor (3,4). Unfortunately, the drugs currently used against various kinases, such as mutant EGFR, are ineffective in patients with lung cancer owing to variable, transient, and incomplete responses (5). Thus, novel therapies are an unmet need for lung cancer patients, in order to improve the progression of the disease.

Anthriscus sylvestris (L.) Hoffm. belongs to the Apiaceae (syn. Umbelliferae) family and grows in hedges, road verges, and neglected pastures in Europe, North America, Asia, and New Zealand (6). In Asia and China, the dried roots of *A. sylvestris* are used in traditional medicine for its antipyretic and analgesic properties and as cough remedy and the young aerial parts are used as food (7). *A. sylvestris* has a high content of lignans. In several studies, monoterpenes, anthricinol, deoxypodophyllotoxin, and angeloylbutenoic acid were separated by hexane-soluble fraction and anthricin, isoanthricin, and crocactone were isolated by EtOAc-soluble fraction (8,9).

Anthricin (deoxypodophyllotoxin) is a major lignan in this plant and has many bioactivities such as antiproliferative, antitumor, anti-platelet aggregation, antiviral, anti-inflammatory and liver protective actions (8,10-12). Numerous studies have reported the anticancer effect of anthricin on various cancer cells, such as gastric and breast cancer, cervical carcinoma and lung cancer, through G2/M cell cycle arrest, microtubule formation inhibition, and caspase-dependent apoptosis (13,14). Jung *et al* reported that anthricin isolated from *A. sylvestris* suppresses the growth of breast cancer cells by inhibiting Akt/mTOR signaling and enhancing autophagy inhibition (15). However, the mechanism underlying this biological phenomenon remains unknown.

Insulin-like growth factor 1 receptor (IGF1R) is a transmembrane receptor tyrosine kinase receptor and highly expressed in various cancers such as lung adenocarcinoma, pancreatic carcinoma, and breast cancer (16). IGF1R signaling on the cell membrane mediated by IGF-1 has a vital role in cell proliferation and differentiation as well as metabolism and against apoptosis (17). When IGF-1 binds to the α domain of IGF1R, the β domain of IGF1R is activated by auto-phosphorylation on specific tyrosine residues and

Correspondence to: Professor Chun Sung Kim, Department of Oral Biochemistry, College of Dentistry, Chosun University, 375 Seosuk-dong, Dong-gu, Gwangju 501-759, Republic of Korea
E-mail: cskim2@chosun.ac.kr

Key words: anthricin, A549 human non-small cell lung cancer cells, IGF1R/PI3K/Akt signaling pathway, cell cycle arrest, apoptosis

switches on the downstream signaling, such as the PI3K/AKT pathway and the RAS/RAF/MEK pathway (18,19). Recently, the clinical significance of IGF1R expression in human NSCLC was reported, and the results revealed that high IGF1R expression on the membranes was predictive of poor progression-free survival (PFS) in adenocarcinoma (20). These findings indicated that IGF1R could be a potential therapeutic target. Thus, we hypothesized that anthricin regulates cell apoptosis through IGF1R/PI3K/AKT signaling. In the present study, we evaluated the effects and mechanism of action of anthricin isolated from *A. sylvestris* in A549 human NSCLC cells.

Materials and methods

Preparation of Anthricin from A. sylvestris (L.) Hoffm. Dried *A. sylvestris* roots were extracted with 10 volumes of methanol (v/w) and the sublayer organic phase was concentrated in a rotary vacuum evaporator (Eyela, Tokyo, Japan) and lyophilized. The residue was dissolved in dimethyl sulfoxide (DMSO), filtered, and analyzed using a Shimadzu HPLC system (Shimadzu Corporation, Kyoto, Japan) consisting of an LC-20AR pump, an SCL 10A system controller and an SPD-20A UV-VIS detector. Semi-preparative HPLC for purification of the methanol extract of dried *A. sylvestris* roots: preparative reversed-phase HPLC was performed using a Shimpack PRC-ODS column (250x20 mm I.D., 5 μm; Shimadzu). The mobile phase was a mixture of two liquids distributed by (A) water and (B) acetonitrile at a flow rate of 1.0 ml/min. The elution program commenced at 95% A: 5% B followed by a linear gradient for 60 min to 5% A: 95% B. The sample injection volume was 1 ml, and the detection by UV was set at a wavelength of 210 nm. Chemical identification was performed by comparing the retention times and mass spectra of the targeted peaks with those of the standard sample. Anthricin (standard sample; Santa Cruz Biotechnology, Inc., Santa Cruz, CA, USA) was dissolved in DMSO at 10 nM, and the anthricin sample prepared from the methanol extract of dried *A. sylvestris* roots was dissolved in DMSO at 10 mg/ml.

Reagents. All the antibodies were purchased from Cell Signaling Technology, Inc. (Beverly, MA, USA), except for β-actin (AB Frontier, Seoul, Korea). A live and dead assay kit and 4,6-dianmidino-2-phenylindole (DAPI) were purchased from Molecular Probes (Carlsbad, CA, USA) and Roche Diagnostics (Bromma, Sweden), respectively. 3-(4,5-Dimethylthiazol-2-yl)-2,5-diphenyltetrazolium bromide (MTT) and propidium iodide (PI) were purchased form Sigma-Aldrich (St. Louis, MO, USA). RPMI-1640 medium and 100 U penicillin-streptomycin solution were purchased from WelGene (Deagu, Korea). Fetal bovine serum (FBS) was purchased from Corning Inc. (Corning, NY, USA). A PE-Annexin V apoptosis detection kit was purchased from BD Biosciences (Franklin Lakes, NJ, USA).

Cell culture. A549 human NSCLC cells were purchased from the Korean Cell Line Bank (Seoul, Korea). Cells were cultured in RPMI-1640 medium supplemented with 10% FBS, 100 U penicillin-streptomycin at 37˚C in a 5% CO_2-humidified incubator.

Cell viability assay. The cytotoxicity of anthricin was assessed using the MTT assay. In brief, the cells were seeded into a 12-well plate ($5x10^5$ cells/ml) and allowed to adhere overnight. The cells were then treated with either vehicle DMSO or anthricin (10, 20, 50, 100 and 200 nM) for 24 and 48 h. Following incubation, 100 μl of MTT solution (5 mg/ml) was added to each well and the plate was incubated for 4 h at 37˚C. The resulting formazan crystals were dissolved in DMSO, and the optical density (OD) was assessed at 570 nm using a microplate reader (Bio-Tek Instruments, Winooski, VT, USA). The cell viability rate was calculated using the following equation: means of $OD_{treated}$/means of $OD_{control}$ x 100%.

Live and dead assay and DAPI staining of cells. A549 cells were seeded in a 4-well chamber slide at a density of $1x10^5$ cells/well. After overnight incubation, the cells were treated with different concentrations of anthricin (0, 10, 20 and 50 nM) for 24 h. Following incubation, the treated cells were washed with phosphate-buffered saline (PBS) twice and fixed with 4% formaldehyde in PBS at room temperature for 10 min. Calcein-AM and ethidium bromide homodimer-1 were used to stain live and dead cells, respectively, according to the manufacturer's instructions. For DAPI staining, the treated cells were washed, fixed with 4% formaldehyde in PBS at room temperature for 10 min, and stained with 300 nM DAPI for 20 min at room temperature. The stained cells were washed thrice with PBS and observed under a fluorescence microscope (Eclipse TE2000; Nikon Instruments, Melville, NY, USA). Cells exhibiting condensed and fragmented nuclei were considered to have undergone apoptosis.

Flow cytometric analysis. A549 cells were treated with anthricin at concentrations of 0, 10, 20 and 50 nM for 24 h, harvested, and washed with ice-cold PBS twice. For the apoptosis analysis, the cells were stained using a PE-Annexin V/7-AAD apoptosis detection kit (BD Biosciences) according to the manufacturer's protocol and subsequently analyzed by flow cytometry (BD FACSCalibur). The quantitative data was expressed as density plots using WDI software. Non-stained cells (Annexin V and 7-AAD negative) were considered viable, cells stained with Annexin V positive and 7-AAD negative were regarded as early apoptotic cells, and cells stained with both Annexin V and 7-AAD were considered late apoptotic or already dead cells. For cell cycle analysis, after cells were treated with anthricin for 24 h, as previously described, they were harvested and washed in ice-cold PBS. The cell pellets were fixed with 4% formaldehyde in PBS for 15 min and stained with 50 μg/ml propidium iodide and 100 μg/ml RNase for 20 min. The data were analyzed using Attune NxT Acoustic Focusing Cytometer (Thermo Fisher Scientific, Inc., Waltham, MA, USA).

Western blot analysis. A549 cells were treated with anthricin at concentrations of 0, 10, 20 and 50 nM for 24 h. The cells were lysed with protein extraction reagent (iNtRON Biotechnology, Sungnam, Korea) for 30 min on ice. The supernatant was transferred to a new tube after centrifugation at 13,000 x g for 15 min at 4˚C (Sorvall Centrifuge, Bad Homburg, Germany). Then, the protein concentrations were quantified using the BCA protein assay (Pierce; Thermo Fisher Scientific, Inc., Waltham, MA, USA) with bovine serum albumin (BSA) as a standard.

Equal amounts of protein (20 μg/lane) were separated by 8 or 15% SDS-PAGE gels under reducing conditions, followed by electrophoretic transfer onto polyvinylidene difluoride (PVDF) membranes (Bio-Rad Laboratories, Hercules, CA, USA). The membranes were blocked with 5% BSA for 1 h. The membranes were incubated at 4˚C overnight with the following primary antibodies diluted to 1:1,000: Bax (cat. no. 2772), Bcl-2 (cat. no. 2872), cleaved caspase-8 (cat. no. 9496), cleaved caspase-3 (cat. no. 9661), cleaved caspase-9 (cat. no. 7237), PARP (cat. no. 9542), Cdc2 (cat. no. 28439), Cdc25C (cat. no. 4688), p-IGF1R(Y1131) (cat. no. 9750), IGF1R (cat. no. 3021), PI3K (cat. no. 4292), p-PI3K (cat. no. 4228), AKT (cat. no. 9272), p-AKT (cat. no. 9271), mTOR (cat. no. 2972), p-mTOR (cat. no. 2971) (all from Cell Signaling Technology, Beverly, MA, USA) and β-actin (1:5,000; cat. no. YIF-LF-PA0207A; AB Frontier, Seoul, Korea). After washing with Tris-buffered saline and Tween-20 (TBST) thrice, the membranes were incubated for 1 h at room temperature with HRP-labeled secondary antibodies, anti-rabbit IgG (cat. no. 7074) and anti-mouse IgG (cat. no. 7076) diluted to 1:5,000 from Cell Signaling Technology. The proteins were detected using Immobilon Western Chemiluminescent HRP Substrate (ECL; Millipore, Bedford, MA, USA) and visualized using a MicroChemi 4.2 device (DNR Bioimaging Systems, Jerusalem, Israel). The density of each band was quantified using ImageJ software and β-actin was used as the internal control.

Mouse xenograft tumor model. Male BALB/c nude mice at four weeks of age were purchased from Damool Science (Daejeon, Korea). Animals were housed in microisolator ventilated cages with environmentally controlled temperature (21±1˚C) and humidity (55±5%), and a reversed 12-h light-dark cycle. Water and food were autoclaved and provided *ad libitum*. All animal experiments were conducted in accordance with the National Institutes of Health (NIH) Care and Use of Laboratory Animals (21) and were approved by the Chosun University Institutional Animal Care and Use Committee (CIACUC2016-S0040). After one week of acclimatization to the laboratory environment, the mice were subcutaneously inoculated with 0.1 ml of PBS containing A549 cells ($1x10^7$ cells/mouse) into the right ear. When the xenograft tumors were palpable and the tumor volume reached ~100 mm^3, the mice were randomly assigned to the control and treatment groups (n=3). Mice received either 10% DMSO in normal saline (control) or anthricin (10 and 20 mg/kg body weight) by intraperitoneal injection every three days. The tumor volume and body weight of the animals were assessed every five days. The tumor volume (V) was calculated by measuring two perpendicular diameters (a, length; b, width) using an electronic digital caliper and the formula used according to the National Cancer Institute (22) was as follows: V (mm^3) = (a x b^2)/2. At the end of the treatment period, all mice were sacrificed under CO_2 and the transplanted tumors were excised and weighed.

Statistical analysis. All data were derived from at least three independent experiments (except the *in vivo* study). Results were expressed as the means ± standard deviation (SD). One-way ANOVA followed by Dunnett's t-test was employed for multiple comparisons using GraphPad Prism (GraphPad Software, Inc., La Jolla, CA, USA). Statistical significance was set at $P<0.05$.

Results

Identification of the main components in the methanol extract of dried A. sylvestris roots by HPLC. The chromatograms revealed the presence of anthricin in the methanol extract of *A. sylvestris* roots (Fig. 1). It was identified by comparing the retention time and UV spectra of the standard sample. The retention time of anthricin was 49.20 min. In Fig. 1B and C, the first peak was ignored as the solvent peak.

Cytotoxic effect of anthricin on A549 cells. To assess the effect of anthricin on cell viability, the cells were treated with anthricin (0, 10, 20, 50, 100 and 200 nM) for the indicated time-points and were analyzed by MTT assay. As shown in Fig. 2, anthricin markedly increased the cytotoxicity of A549 cells in a dose- and time-dependent manner. Since anthricin exhibited cytotoxicity at 10 nM in 24 h, further experiments were performed at 10, 20 and 50 nM.

Induction of apoptosis by anthricin in A549 cells. To determine whether cytotoxicity of anthricin was related to apoptosis, we investigated induction of apoptosis of A549 cells by anthricin using a live and dead assay, DAPI staining, FACS analysis, and western blotting. As shown in Fig. 3A, cells stained with ethidium bromide homodimer-1 (dead dye, red color) gradually increased with anthricin treatment dose-dependently. In addition, anthricin-treated cells exhibited a significant increase in the apoptotic cell population compared with the control. Cells stained brightly by nuclear condensation were considered as apoptotic cells. Based on the apoptosis phenomenon of anthricin observed in the live and dead assay and DAPI staining (Fig. 3A and B, respectively), we performed FACS analysis for the quantification of apoptotic cells. A549 cells were treated with anthricin as previously indicated and then double-stained with PE-Annexin V/7-AAD. The percentage of Annexin V-positive apoptotic cells increased to 13.52, 14.7 and 23.94% at 10, 20 and 50 nM anthricin, respectively, compared with the control (0.09%) (Fig. 3C). Western blotting was performed to evaluate whether A549 cell apoptosis induced by anthricin was dependent on caspases. As shown in Fig. 3E, the cleavage of caspase-8, -3 and -9 significantly increased in a dose-dependent manner and thus the cleavage of native PARP (116 kDa) into its small fragment PARP (89 kDa) increased. Furthermore, anthricin-mediated apoptosis was associated with the outer mitochondrial membrane in a dose-dependent manner. Anti-apoptotic Bcl-2 protein levels decreased but anti-survival Bax protein levels increased (Fig. 3D). Collectively, these results revealed that anthricin-induced apoptosis of A549 cells may be mediated by the activation of caspase in the extrinsic death receptor and intrinsic mitochondrial-dependent apoptotic signaling pathways.

Induction of cell cycle arrest by anthricin in A549 cells. Flow cytometric analysis revealed that the percentage of cells in the G2/M phase increased in anthricin-treated cells compared with the control (Fig. 4A and B). This peak markedly

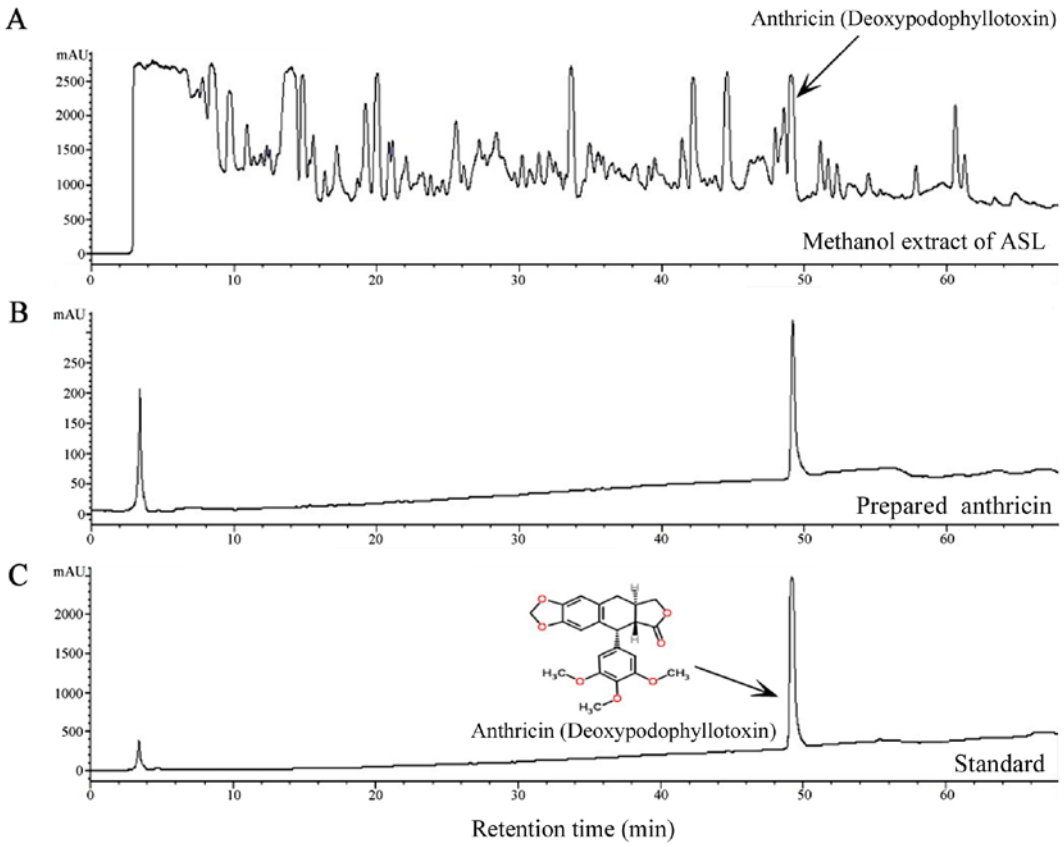

Figure 1. HPLC chromatograms of the methanol extract of the dried *A. sylvestris* root. (A and B) HPLC chromatograms of (A) the methanol extract of the dried *A. sylvestris* root at 10 mg/ml and (B) prepared anthricin were identified at 210 nm. (C) HPLC chromatograms of the anthricin standard were identified at 210 nm.

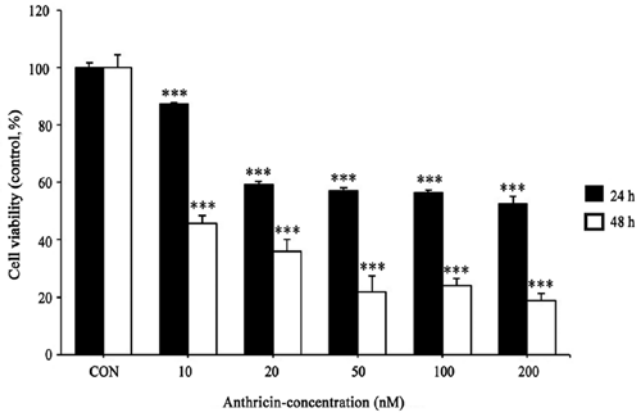

Figure 2. Effect of anthricin on A549 cell viability. Cells were treated with various concentrations of anthricin (0, 10, 20, 50, 100 and 200 nM) for 24 and 48 h. Cell viability was determined using an MTT assay. Results were expressed as the percentage of the control. Data are expressed as the means ± SD of three independent experiments. ***P<0.001 compared with the control group.

increased at 20 and 50 nM anthricin (~81.05 and 68.69%, respectively). In addition, the results for the detected sub-G1 group indicated that anthricin induced apoptosis of A549 cells. Western blot analysis was performed to examine the expression of G2/M-boundary regulatory proteins, including Cdc2 and Cdc25C. As shown in Fig. 4C, the protein expression of Cdc2 and Cdc25C significantly decreased 24 h after anthricin treatment in a dose-dependent manner, indicating that anthricin induces G2/M phase arrest in A549 cells.

Effect of anthricin on the expression of IGF1R, PI3K, and Akt. IGF1R is upregulated in various cancers, including breast, prostate, and lung cancers, and mediates cell cycle progression and prevention of apoptosis in hematopoietic cells (23). Thus, we examined the effects of anthricin on the IGF1R/PI3K/Akt signaling pathways in A549 cells. After 24 h of exposure to anthricin (0, 10, 20 and 50 nM), the protein expression levels of p-IGF1R (Y1131) were reduced to 65, 22 and 3%, at 10, 20 and 50 nM anthricin, respectively (Fig. 5). In addition, anthricin treatment reduced the protein expression levels of p-PI3K (P85) and p-Akt (Ser473), which IGF1R targets downstream in a dose-dependent manner (Fig. 5). As mTOR is a downstream target of the Akt gene, the expression of p-mTOR (Ser2448) was reduced due to the inhibition of Akt (Fig. 5). These results revealed that anthricin induced apoptosis by inhibiting the IGF1R/PI3K/Akt signaling pathways.

Antitumor effect of anthricin in human lung adenocarcinoma cell-derived mouse xenografts in vivo. Based on the aforementioned *in vitro* anticancer effect, we investigated the inhibitory effects of anthricin on A549 xenografts. Mice were injected (i.p.) with 10 and 20 mg/kg of anthricin every three days for 30 days. The tumors removed from these animals

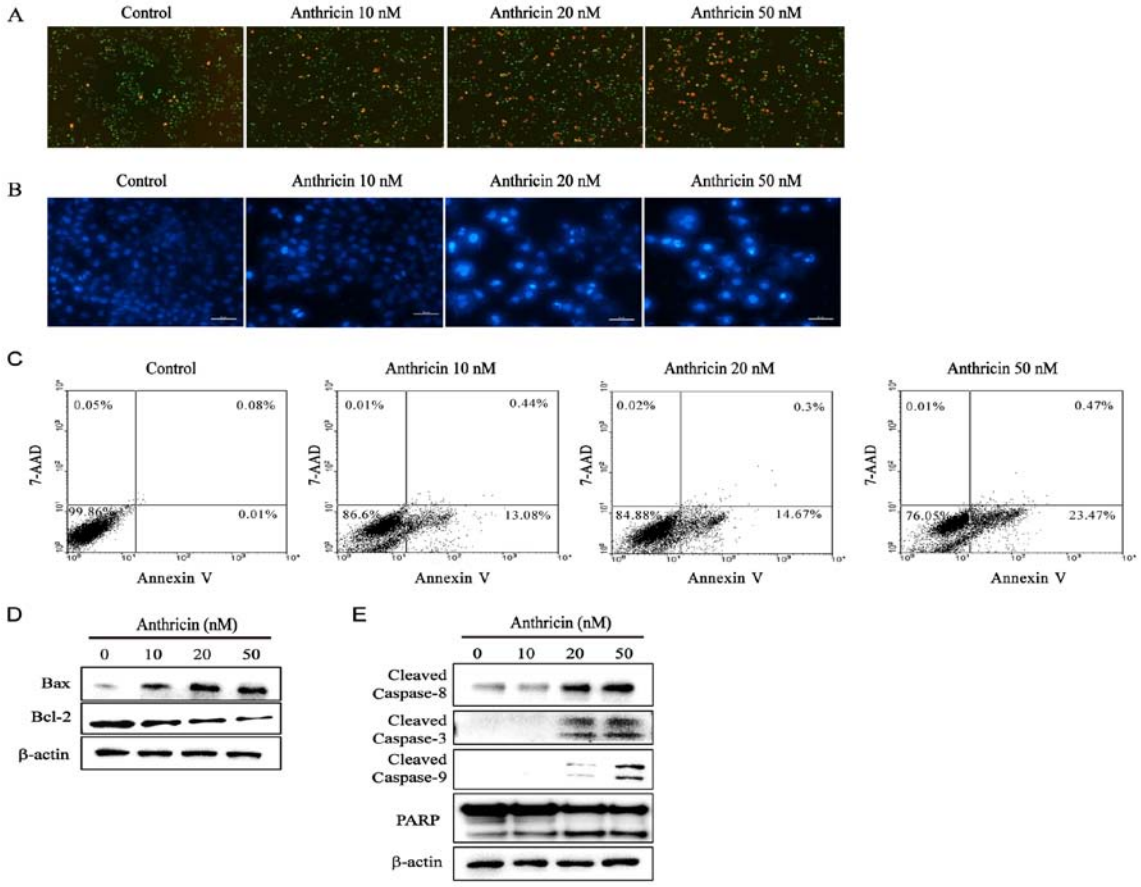

Figure 3. Induction of apoptosis by anthricin in A549 cells. Cells were treated with various concentrations of anthricin (0, 10, 20 and 50 nM) for 24 h. (A) Live and dead cells were stained by calcein-AM and ethidium bromide homodimer-1, respectively. Stained cells were observed by fluorescence microscopic analysis and imaged (magnification, x100). (B) After anthricin treatment, DNA was stained with DAPI and observed by fluorescence microscopic analysis and imaged (magnification, x100). (C) Annexin V/7-AAD double-staining revealed the percentage of apoptotic cells after anthricin treatment. The proportion of cells in each quadrant are marked on the figures. (D and E) After anthricin treatment, the expression of apoptotic-related proteins (cleaved caspase-8, cleaved caspase-3, cleaved caspase-9, PARP, Bax and Bcl-2) was assessed by western blotting, and β-actin was used as the loading control. Data are expressed as the means ± SD of three independent experiments.

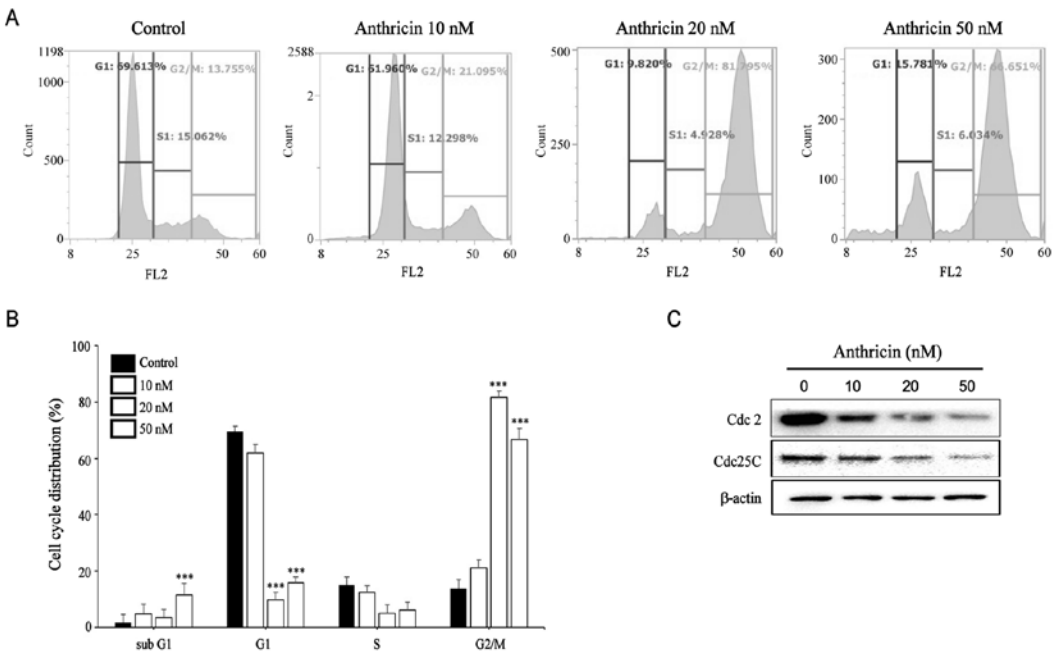

Figure 4. Effect of anthricin on cell cycle distribution in A549 cells. Cells were treated with various concentrations of anthricin (0, 10, 20, and 50 nM) for 24 h. (A) The cell cycle distribution was monitored by flow cytometry. (B) Data are expressed as the mean ± SD (n=3). (C) The expression of cell cycle-related proteins (Cdc2 and Cdc25C) were assessed by western blotting, and β-actin was used as the loading control. Data are expressed as the means ± SD of three independent experiments. ***P<0.001 compared with the control group.

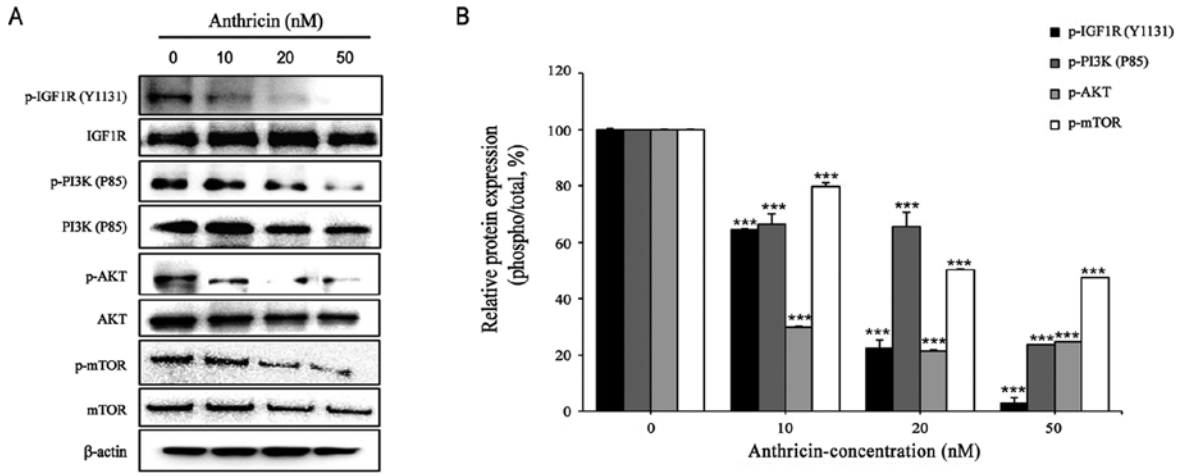

Figure 5. Effect of anthricin on the expression of IGF1R, PI3K, and Akt in A549 cells. Cells were treated with various concentrations of anthricin (0, 10, 20, and 50 nM) for 24 h. (A) The protein expression levels of IGF1R/PI3K/Akt and mTOR were assessed by western blotting, and β-actin or each total form was used as a loading control. (B) The data revealed the relative phospho-form expression of each protein normalized to total-form. Data are expressed as the means ± SD of three independent experiments. ***P<0.001 compared to the control group.

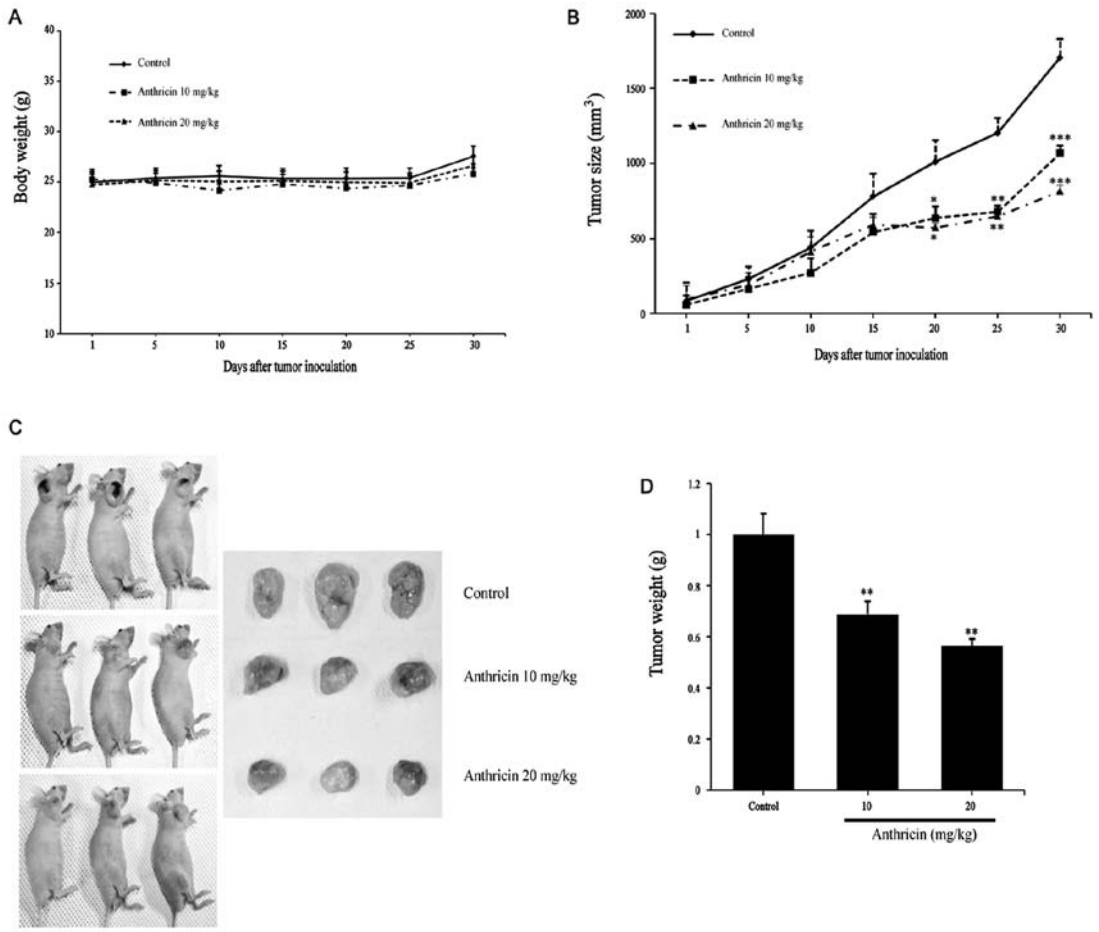

Figure 6. Effects of anthricin on A549 xenograft growth in nude mice. A549 cells were subcutaneously injected in the right ear. The mice were administered 0.1 ml of control (10% DMSO in normal saline) or anthricin (10 and 20 mg/kg body weight) intraperitoneally every three days for 30 days. (A) The change in the body weight of animals. (B) Size of the excised xenograft tumors. Tumor size was measured with a Vernier caliper, and calculated using the equation described in the Materials and methods section. (C) Excised xenograft tumors after 30 days of treatment. (D) Weight (g) of the excised xenograft tumors. *P<0.05, **P<0.01 and ***P<0.001 compared with the control group.

are shown in Fig. 6C, and their size and weight have been provided in Fig. 6C and D, respectively. The tumor growth of A549 xenografts were significantly inhibited by anthricin treatment, and the inhibitory rates were 37.34 and 52.17%, at 10 and 20 mg/kg anthricin, respectively, compared with that in the vehicle-treated animals (Fig. 6B). In addition,

the tumor mean weights were 883.33±41.55, 606.66±18.04 and 496.67±23.84 mg in the control and after treatment with 10 and 20 mg/kg anthricin, respectively; the inhibition rates were 32 and 44% (Fig. 6D). There was no significant difference in body weight between the groups (Fig. 6A) and no sign of skin rash or diarrhea. All animals appeared to be in a decent state despite treatment. These results revealed that anthricin exhibits potential as a novel antitumor therapeutic agent against lung cancer.

Discussion

Anthriscus sylvestris (L.) Hoffm. has been used in traditional medicine as an antipyretic, analgesic agent and as a cough remedy. It contains lignans such as anthricin (7), which is a major lignan in this plant and exhibits antitumor activity in various cancer cells, such as gastric, breast and lung cancer through apoptosis (13,14). In the present study, we isolated anthricin from *A. sylvestris* and investigated the mechanism underlying apoptosis following anthricin treatment in A549 cells. Previous research has reported that anthricin isolated from *A. sylvestris* inhibits the growth of breast cancer cells by inhibiting Akt/mTOR signaling and enhancing autophagy inhibition (15). In addition, anthricin has demonstrated an anticancer effect through cell cycle arrest at the G2/M phase and caspase-mediated apoptosis in gastric, breast and lung cancer cells (15,24,25).

We found *in vitro* that anthricin treatment induced G2/M phase arrest and caspase-mediated apoptosis in A549 cells. Our data revealed that anthricin treatment strongly inhibited A549 cell viability in a dose- and time-dependent manner and that the suppression of cell viability was due to cell cycle arrest at the G2/M phase. Following 24 h of anthricin exposure, most cells were arrested at the G2/M phase and there was a slight increase in the sub-G1 cell population, as indicated by flow cytometric analysis. Western blot analysis was carried out to examine the mechanism of cell cycle progression and it was revealed that anthricin decreased the expression of Cdc2 and Cdc25C. Cdc2 forms maturation promoting factor (MPF), which regulates the transition from the G2 to the M phase through interaction with cyclin B1 (26). Cdc25C regulates the subsequent activation of the cyclin B1/Cdc2 complex by inhibiting phosphorylation of Cdc2 on Thr14/Tyr15. These results revealed that anthricin induced cell cycle arrest at the G2/M phase by suppressing the cell cycle regulators Cdc2 and Cdc25C. This was consistent with previous studies which revealed that anthricin induced cell cycle arrest at the G2/M phase in H460 lung cancer cells and HeLa cancer cells (13,25). Since the cell population in sub-G1, the hallmark of apoptotic cell death, increased after anthricin exposure, we investigated anthricin-induced apoptosis. We found that anthricin-induced apoptosis was mediated through a caspase-dependent pathway. Shin *et al*, reported that anthricin induced caspase-dependent apoptosis after G2/M cell cycle arrest in HeLa cervical cancer cells (13). In addition, Wang *et al*, suggested that G2/M phase arrest occurred in SGC-7901 cells, a gastric cancer cell line, after exposure to 50 nM anthricin and then apoptosis was induced through the activation of caspases (24).

To analyze the mechanism underlying anthricin-induced apoptosis, we investigated the expression of IGF1R by western blotting. IGF1R is induced by many oncogenes and strongly overexpressed in several types of tumors, including ovarian, prostate, breast, and lung tumors (27,28). Recently, Yeo *et al*, reported that high expression of the IGF1R protein was a negative predictor of response to EGFR-directed treatment and was associated with poor PFS in EGFR-mutated NSCLC patients (28,29). IGF1R pathways play a crucial role in cell proliferation and differentiation and against apoptosis through the activation of the RAS/RAF/MEK and PI3K/Akt pathways (23). The PI3K/Akt pathway is of high interest among many canonical pathways in cancer development and maintenance (30). PI3K phosphorylates PIP2 and PIP3 and in turn phosphorylates Akt. Akt, activated by phosphorylation at the Ser473 residue, stimulates mTOR complex 1 (mTORC1), and mTORC1 phosphorylates mTOR at Ser2448 (31). Our results revealed that anthricin inhibited the phosphorylation of IGF1R at the Tyr 1131 residue, thereby inhibiting the phosphorylation of PI3K and AKT, which is downstream of IGF1R. These results were consistent with those of previous studies which revealed that anthricin isolated from *A. sylvestris* inhibits the growth of breast cancer cells by inhibiting Akt/mTOR signaling (15). In addition, Hu *et al*, reported that anthricin induced apoptosis of human prostate cancer cells through the Akt/p53/Bax/PTEN signaling pathways (32). To the best of our knowledge, the involvement of IGF1R in anthricin-induced cell apoptosis of A549 cells has been reported for the first time.

In *in vivo* experiments, anthricin at 10 and 20 mg/kg inhibited tumor growth without any significant changes in the body weight of mice. Previous studies reported that the antitumor activity of anthricin at 10 and 20 mg/kg was more pronounced than that of etoposide or docetaxel without any side-effects in NCL-H460 lung cancer cells and SGC-7901 gastric cancer cells (24,25).

In conclusion, this study revealed, for the first time, that anthricin-induced apoptosis was mediated by the IGF1R/PI3K/Akt signaling pathway in A549 cells. We believe that this study provided meaningful insights. However, the relationship between anthricin and IGF1R warrants further investigation.

Acknowledgements

Not applicable.

Funding

The present study was supported by a research funding from the Chosun University (2014).

Availability of data and materials

The datasets used during the present study are available from the corresponding author upon reasonable request.

Author's contributions

CSK and SMM conceived and designed this study. SMM analyzed the HPLC analysis and prepared sample (anthricin).

BRP and SAL performed the all *in vitro* experiments. BRP performed the *in vivo* experiments and wrote the manuscript. CSK reviewed and edited the manuscript. All authors read and approved the manuscript and agree to be accountable for all aspects of this research in ensuring that the accuracy or integrity of any part of the work are appropriately investigated and resolved.

Ethics approval and consent to participate

All experimental protocols were approved by the Institutional Animal Care and Use Committee of Chosun University (CIACUC2016-S0040).

Consent for publication

Not applicable.

Competing interests

The authors declare that they have no competing interests.

References

1. Field JK and Duffy SW: Lung cancer screening: The way forward. Br J Cancer 99: 557-562, 2008.
2. Gu JJ, Rouse C, Xu X, Wang J, Onaitis MW and Pendergast AM: Inactivation of ABL kinases suppress non-small cell lung cancer metastasis. JCI Insight 1: e89647, 2016.
3. Poomakkoth N, Issa A, Abdulrahman N, Abelaziz SG and Mraiche F: p90 ribosomal S6 kinase: A potential therapeutic target in lung cancer. J Transl Med 14: 14, 2016.
4. Li T, Kung HJ, Mack PC and Gandara DR: Genotyping and genomic profiling of non-small-cell lung cancer: Implications for current and future therapies. J Clin Oncol 31: 1039-1049, 2013.
5. Gridelli C, Bareschino MA, Schettino C, Rossi A, Maione P and Ciardiello F: Erlotinib in non-small cell lung cancer treatment: Current status and future development. Oncologist 12: 840-849, 2007.
6. Olaru OT, Nitulescu GM, Ortan A and Dinu-Pirvu CE: Ethnomedicinal, Phytochemical and Pharmacological profile of Anthriscus sylvestris as an alternative source for anticancer lignans. Molecules 20: 15003-15022, 2015.
7. Kozawa M, Baba K, Matsuyama Y, Kido T, Sakai M and Takemoto T: Components of the root of Anthriscus sylvestris Hoffm. II. Insecticidal activity. Chem Pharm Bull 30: 2885-2888, 1982.
8. Kozawa M, Morita N and Hata K: Chemical components of the roots of Anthriscus sylvestris Hoffm. L. structures of an acyloxycarboxylic acid and a new phenylpropanoidester, anthriscusin (authour's transl). Yakugaku Zasshi 98: 1486-1490, 1978 (In Japanese).
9. Kurihara T, Kikuchi M, Suzuki S and Hisamichi S: Studies on the constituents of Anthriscus sylvestris Hoffm. L. On the components of the radix (authour's transl) Yakugaku Zasshi 98: 1586-1597, 1978 (In Japanese).
10. Lim YH, Leem MJ, Shin DH, Chang HB, Hong SW, Moon EY, Lee DK, Yoon SJ and Woo WS: Cytotoxic constituents from the roots of Anthriscus sylvestris. Arch Pharm Res 22: 208-212, 1999.
11. Jin M, Moon TC, Quan Z, Lee E, Kim YK, Yang JH, Suh SJ, Jeong TC, Lee SH, Kim CH and Chang HW: The naturally occurring flavolignan, deoxypodophyllotoxin, inhibits lipopolysaccharide-induced iNOS expression through the NF-kappaB activation in RAW264.7 macrophage cells. Biol Pharm Bull 31: 1312-1315, 2008.
12. Kiso Y, Konno C, Hikino H, Yagi Y and Hashimoto I: Liver-protective actions of desoxypodophyllotoxin and its analogs. J Pharmacobiodyn 5: 638-641, 1982.
13. Shin SY, Yong YJ, Kim CG, Lee YH and Lim Y: Deoxypodophyllotoxin induces G2/M cell cycle arrest and apoptosis in HeLa cells. Cancer Letter 287: 231-239, 2010.
14. Jiang Z, Wu M, Miao J, Duan H, Zhang S, Chen M, Sun L, Wang Y, Zhang X, Zhu X and Zhang L: Deoxypodophyllotoxin exerts both anti-angiogenic and vascular disrupting effects. Int J Biochem Cell Biol 45: 1710-1719, 2013.
15. Jung CH, Kim HM, Ahn JY, Jung SK, Um MY, Son KH, Kim TW and Ha TY: Anthricin isolated from *Anthriscus sylvestris* (L.) Hoffm. inhibits the growth of breast cancer cells by inhibiting Akt/mTOR signaling, and its apoptotic effects are enhanced by autophagy inhibition. Evid Based Complement Alternat Med 2013: 385219, 2013.
16. Baserga R, Peruzzi F and Reiss K: The IGF-1 receptor in cancer biology. Int J Cancer 107: 873-877, 2003.
17. Laron Z: Insulin-like growth factor 1 (IGF-1): A growth hormone. Mol Pathol 54: 311-316, 2001.
18. Iams WT and Lovly CM: Molecular pathways: Clinical applications and future direction of insulin-like growth factor-1 receptor pathway blockade. Clin Cancer Res 21: 4270-4277, 2015.
19. King H, Aleksic T, Haluska P and Macaulay VM: Can we unlock the potential of IGF-1R inhibition in cancer therapy? Cancer Treat Rev 40, 1096-1105, 2014.
20. Park E, Park SY, Kim H, Sun PL, Jin Y, Cho SK, Kim K, Lee CT and Chung JH: Membranous insulin-like growth factor-1 receptor (IGF1R) expression is predictive of poor prognosis in patients with epidermal growth factor receptor (EGFR)-mutant lung adenocarcinoma. J Pathol Transl Med 49: 382-388, 2015.
21. National Research Council: Guide for the care and use of laboratory animals. In: National Academies Press. Eight (ed), Washington DC, 2011.
22. Geran RI, Greenberg NH, McDonald MM, Schumacher A and Abbott BJ: Protocols for screening chemical agents and natural products against animal tumours and other biological system. Cancer Chemother Rep 3: 51-61, 1972.
23. Bertrand FE, Steelman LS, Chappell WH, Abrams SL, Shelton JG, White ER, Ludwig DL and McCubrey JA: Synergy between an IGF 1R antibody and Raf//MEK//ERK and PI3K//Akt//mTOR pathway inhibitors in suppressing IGF 1R mediated growth in hematopoietic cells. Leukemia 20: 1254 1260, 2006.
24. Wang YR, Xu Y, Jiang ZZ, Guerram M, Wang B, Zhu X and Zhang LY: Deoxypodophyllotoxin induces G2/M cell cycle arrest and apoptosis in SGC-7901 cells and inhibits tumor growth in vivo. Molecules 20: 1661-1675, 2015.
25. Wu M, Jiang Z, Duan H, Sun L, Zhang S, Chen M, Wang Y, Gao Q, Song Y, Zhu X and Zhang L: Deoxypodophyllotoxin triggers necroptosis in human non-small cell lung cancer NCL-J460 cells. Biomed Pharmacother 67: 701-706, 2013.
26. Graña X and Reddy EP: Cell cycle control in mammalian cells: Role of cyclins, cyclin dependent kinases (CDKs), growth suppressor genes and cyclin-dependent kinase inhibitors (CKIs). Oncogene 11: 211-219, 1995.
27. Wang Y and Sun Y: Insulin-like growth factor receptor-1 as an anti-cancer target: Blocking transformation and inducing apoptosis. Curr Cancer Drug Targets 2: 191-207, 2002.
28. Hewish M, Chau I and Cunningham D: Insulin-like growth factor 1 receptor targeted therapeutics: Novel compounds and novel treatment strategies for cancer medicine. Recent Pat Anticancer Drug Discov 4: 54-72, 2009.
29. Yeo CD, Park KH, Park CK, Lee SH, Kim SJ, Yoon HK, Lee YS, Lee EJ, Lee KY and Kim TJ: Expression of insulin-like growth factor 1 receptor (IGF-1R) predicts poor responses to epidermal growth factor receptor (EGFR) tyrosine kinase inhibitors in non-small cell lung cancer patients harboring activating EGFR mutations. Lung Cancer 87: 311-317, 2015.
30. van der Wekken AJ, Saber A, Hiltermann TJ, Kok K, van den Berg A and Groen HJ: Resistance mechanisms after tyrosine kinase inhibitors afatinib and crizotinib in non-small cell lung cancer, a review of the literature. Crit Re Oncol Hematol 100: 107-116, 2016.
31. Singh SS, Yap WN, Arfuso F, Kar S, Wang C, Cai W, Dharmarajan AM, Sethi G and Kumar AP: Targeting the PI3K/Akt signaling pathway in gastric carcinoma: A reality for personalized medicine? World J Gastroenterol 21: 12261-12273, 2015.
32. Hu S, Zhou Q, Wu WR, Duan YX, Gao ZY, Li YW and Lu Q: Anticancer effect of deoxypodophyllotoxin induces apoptosis of human prostate cancer cells. Oncol Lett 12: 2918-2923, 2016.